



# An effective method for calculation of diffusive flow in spherical grains

P. Hermansson<sup>a,\*</sup>, A.R. Massih<sup>b,c</sup>

<sup>a</sup> FOI, P.O. Box 1165, SE-581 11 Linköping, Sweden

<sup>b</sup> Quantum Technologies AB, Uppsala Science Park, SE-751 83 Uppsala, Sweden

<sup>c</sup> Malmö University, SE-205 06 Malmö, Sweden

Received 22 February 2002; accepted 17 April 2002

## Abstract

The accuracy of a numerical fission gas release algorithm developed by Forsberg and Massih for solving the problem of diffusive flow to a spherical grain boundary is analysed. Estimates of numerical errors are derived for both steady-state and time varying conditions. We also present a method through which the accuracy of the algorithm can be improved or optimised for most applications.

© 2002 Elsevier Science B.V. All rights reserved.

## 1. Introduction

The evaluation of the behaviour of fission product gases in nuclear fuel is an important aspect of fuel rod design and safety analysis [1]. The fission gases xenon and krypton, generated during fissioning of uranium and plutonium isotopes or through nuclear decay processes, diffuse inside grains of UO<sub>2</sub> fuel and precipitate into intra- and intergranular gas bubbles. Grain boundary gas bubble saturation (through bubble interlinkage) eventually leads to release of fission product gases to the free volume of fuel rod. The fission gas release calculation method has a central role in fuel rod behaviour codes (see, e.g. [2,3]). The common assumption in many calculations is the concept of the equivalent sphere model. This notion considers the polycrystalline sinter as a collection of spheres of uniform size characterised by a single radius  $a$ .

Nuclear fuel during reactor operation is subject to time-varying power histories both under normal operation and in operational transients. This makes the physical parameters entering the governing equations for gas diffusion in fuel grains time dependent. Thus an

efficient algorithm for solving the diffusion equation, with a time-dependent diffusion coefficient and source term in a spherical grain, is important for computing fission gas release in nuclear fuel behaviour codes.

Noble and Rim [4] obtained an exact solution for the case of stepwise time varying conditions. However, this method requires quite long computing times. Using a variational principle, Matthews and Wood [5] derived a more rapid algorithm for solving the diffusion problem. Forsberg and Massih [6,7] presented an alternative rapid and economical algorithm, using the method of an approximating kernel. Elton and Lassmann [8] evaluated the accuracy of several fission gas release algorithms, including the Forsberg–Massih algorithm, by calculating the errors for a large number of random operating histories. Elton and Lassmann noted that the Forsberg–Massih fission gas release algorithm has rather large systematic errors at low fission gas release. More recently, Lassmann and Benk [9] have reviewed and analysed various numerical algorithms for intragranular fission gas release. They conclude that although the Forsberg–Massih algorithm can be considered to be ‘exact’ for gas release fractions above 0.05, for low release fractions it gives a systematic over-prediction. Furthermore, they improved the accuracy of the original Forsberg–Massih algorithm by slightly modifying that

\* Corresponding author.

algorithm, which they called new FORMAS algorithm. We believe that the inaccuracy in the original Forsberg–Massih algorithm chiefly stems from the choice of fitting coefficients appearing in the approximate solution and not from the framework of the algorithm.

In this note we will derive some estimates of numerical errors in the Forsberg–Massih fission gas release algorithm. Based on these results we will suggest a method through which the accuracy of the algorithm can be improved (or optimised) for most types of application. Finally, we present two examples of approximate kernels, which improve the accuracy of the Forsberg–Massih algorithm.

## 2. The model

### 2.1. The diffusion equation and its formal solution

In the modelling of diffusive fission gas release in nuclear fuel one assumes that the medium for gas diffusion is an equivalent idealized spherical grain for which the governing equation for concentration of gas atoms is expressed by

$$\frac{\partial c(r, t)}{\partial t} = D_e(t) \nabla_r^2 c(r, t) + \beta(t) \quad (1)$$

with the Laplacian operator:

$$\nabla_r^2 \equiv \frac{\partial^2}{\partial r^2} + \frac{2}{r} \frac{\partial}{\partial r}.$$

Here  $c(r, t)$  is the local concentration of fission gas,  $t$  is the time,  $r$  is the radial coordinate in spherical coordinates,  $\beta(t)$  is the rate at which gas is produced,  $D_e(t)$  is the effective gas diffusion coefficient [10] and  $a$  is the equivalent grain size. The initial condition imposed on Eq. (1) can be either  $c(r, 0) = 0$  or  $c(r, 0) = c(r)$ . The boundary condition in Eq. (1) can be the perfect sink boundary condition, where all the gas reaching the grain boundary will be released, i.e., the Dirichlet condition:

$$c(a, t) = 0. \quad (2)$$

If we cater for the presence of intergranular gas and resolution at the grain boundaries [10], the Cauchy condition prevails:

$$c(a, t) = b(t) \lambda N(t) / 2D_e(t), \quad (3)$$

where  $b$  is the re-resolution rate,  $\lambda$  the re-resolution distance (from the grain boundary) and  $N$  is the number of gas atoms (in bubbles) per unit area of grain boundary. In addition, the Neumann symmetry condition,  $\partial c(r, t) / \partial r|_{r=0} = 0$ , always must be fulfilled by Eq. (1).

Eq. (1) can be transformed to [6]

$$\frac{\partial c(r, \tau)}{\partial \tau} = \nabla_r^2 c(r, \tau) + \frac{\tilde{\beta}(\tau)}{\tilde{D}_e(\tau)} \quad (4)$$

by making use of the co-ordinate transformation

$$\tau = \int_0^t D_e(t) dt,$$

where the transformation is a diffeomorphism if  $D_e > 0$  and  $D_e$  is a continuous function, or more precisely,  $\tilde{D}_e(\tau) \in C^0$ ; also  $c(r, t(\tau)) \rightarrow c(r, \tau)$ ,  $\tilde{D}_e(\tau) = D_e(t(\tau))$  and  $\tilde{\beta}(\tau) = \beta(t(\tau))$ , for definitions see mathematical physics texts, e.g. [11]. Similarly the boundary conditions (2) and (3) in the  $\tau$ -space become, respectively

$$c(a, \tau) = 0, \quad (5)$$

$$c(a, \tau) = \tilde{b}(\tau) \lambda \tilde{N}(\tau) / 2\tilde{D}_e(\tau), \quad (6)$$

where  $\tilde{N}(\tau) = N(t(\tau))$  and  $\tilde{b}(\tau) = b(t(\tau))$ . The average gas concentration (per unit volume) in the grain of radius  $a$  is given by  $\bar{c}(\tau) = (3/a^3) \int_0^a r^2 c(r, \tau) dr$ . Expanding Eq. (4) in terms of the eigenfunctions of the Laplacian operator, for the perfect sink boundary condition, Eq. (5), we obtain [6]

$$\bar{c}(\tau) = \frac{3}{4\pi} \int_0^\tau K\left(\frac{\tau-s}{a^2}\right) P(s) ds, \quad (7)$$

where  $P(s) = \tilde{\beta}(s) / \tilde{D}_e(s)$  and the kernel  $K(x)$  is given by

$$K(x) = \frac{8}{\pi} \sum_{k=1}^{\infty} \frac{e^{-k^2 \pi^2 x}}{k^2}. \quad (8)$$

The fission gas release fraction,  $\mathfrak{R}$ , is defined by

$$\mathfrak{R}(\tau) = 1 - \frac{\bar{c}(\tau)}{\bar{c}_c(\tau)}, \quad (9)$$

where

$$\bar{c}_c(\tau) = \int_0^{t(\tau)} \beta(s) ds = \int_0^\tau P(s) ds. \quad (10)$$

For the Cauchy boundary condition, Eq. (6), the areal gas density on the grain boundary is expressed as [7]

$$\tilde{N}(\tau) = 2 \int_0^\tau K_2\left(\frac{\tau-s}{a^2}\right) \left[ P(s) - \frac{1}{2} \frac{d}{ds} \left( \frac{\tilde{b}(s) \lambda \tilde{N}(s)}{\tilde{D}_e(s)} \right) \right] ds, \quad (11)$$

where

$$K_2(x) = \frac{a}{3} \left( 1 - \frac{3K(x)}{4\pi} \right). \quad (12)$$

### 2.2. Incremental algorithm using an approximate kernel

In Forsberg and Massih [6] the kernel  $K(x)$  in Eq. (8) is approximated by

$$K(x) \approx \tilde{K}(x) = \sum_{i=1}^m A_i e^{-B_i x}. \quad (13)$$

It is clear that Eq. (13) can approximate  $K(x)$  to any order of accuracy by increasing the number of terms  $m$ . The advantage of using an approximate kernel of the form (13) is that it readily leads to an incremental algorithm for calculation of  $\bar{c}$ . Inserting the approximate kernel (13) in Eq. (7) and assuming that  $P(s) \approx \bar{P} = \text{constant}$  in the interval  $[\tau, \tau + \Delta\tau]$ , we get the incremental algorithm (cf. [9])

$$\bar{c}_i(\tau + \Delta\tau) = \frac{3}{4\pi} \left[ e^{-B_i \Delta\tau/a^2} \left( \frac{4\pi}{3} \bar{c}_i(\tau) - \frac{A_i a^2}{B_i} \bar{P} \right) + \frac{A_i a^2}{B_i} \bar{P} \right], \quad (14)$$

where  $\bar{c}(\tau) = \sum_{i=1}^m \bar{c}_i(\tau)$  is the average gas concentration per unit volume of the grain.

In Forsberg and Massih [6]  $P(\tau)$  was taken to be piecewise linear, i.e.,  $P(s) \approx P(\tau + \Delta\tau) + (s - \tau - \Delta\tau)h$ , where  $h = (P(\tau + \Delta\tau) - P(\tau))/\Delta\tau$  in the interval  $(\tau, \tau + \Delta\tau)$ . This choice leads to the relation

$$c_i(\tau + \Delta\tau) = \frac{3}{4\pi} \left[ e^{-B_i \Delta\tau/a^2} \left( \frac{4\pi}{3} c_i(\tau) + \frac{a^2 A_i}{B_i} \left( \frac{a^2 h}{B_i} - P(\tau) \right) \right) - \frac{a^2 A_i}{B_i} \left( \frac{a^2 h}{B_i} - P(\tau + \Delta\tau) \right) \right]. \quad (15)$$

### 3. Steady-state condition

In order to evaluate the accuracy of the foregoing algorithm it is useful to have an exact solution. Assuming a steady-state condition, under which the gas production rate, the gas diffusion coefficient and the re-solution rate are time independent, exact analytical solutions for the considered governing equations, Eqs. (7) and (11), can be found. In this section we present these relations for the two cases under consideration, namely, (i) the perfect sink boundary condition (Dirichlet), also referred to as the intragranular gas release, and (ii) the grain boundary gas accumulation and the re-solution effect (Cauchy boundary condition), alluded to as the intergranular gas release.

#### 3.1. Dirichlet boundary condition

Let us consider the case that the gas production term is constant, more precisely the ratio  $P(s) = \tilde{\beta}(s)/\tilde{D}_e(s) \equiv \bar{P} = \text{constant}$ . Then using the identity  $\sum_{k=1}^{\infty} k^{-4} = \pi^4/90$ , Eq. (7) can be integrated and the result, in terms of the fission gas release fraction, Eq. (9), is expressed as

$$\mathfrak{R}(\tau) = 1 - \frac{a^2}{15\tau} \left[ 1 - \frac{90}{\pi^4} \sum_{k=1}^{\infty} \frac{e^{-k^2 \pi^2 \tau/a^2}}{k^4} \right]. \quad (16)$$

For the approximate solution, relation (13), the gas release fraction under steady-state condition is expressed by

$$\mathfrak{R}(\tau) \approx \tilde{\mathfrak{R}}(\tau) = 1 - \frac{3a^2}{4\pi\tau} \left[ \sum_{i=1}^m \frac{A_i}{B_i} \left( 1 - e^{-B_i \tau/a^2} \right) \right]. \quad (17)$$

After determining the coefficients  $A_i$  and  $B_i$  we shall compare Eq. (16) with Eq. (17) to assess the level of our approximation.

#### 3.2. Cauchy boundary condition

For the case of grain boundary gas accumulation the steady-state condition entails that the gas production rate, diffusion coefficient and the re-solution rate are constant with time. Here, however, we obtain exact relations when the ratios  $\tilde{\beta}(\tau)/\tilde{D}_e(\tau)$  and  $\tilde{b}(\tau)\lambda/\tilde{D}_e(\tau)$  are time independent, which provide, as the condition in Section 3.1, a more general situation than steady-state. The governing equation (11) for the kinetics of gas concentration on the grain boundary becomes

$$\tilde{N}(\tau) = 2 \int_0^\tau K_2 \left( \frac{\tau - s}{a^2} \right) \left[ \bar{P} - \frac{h_1}{2} \frac{d\tilde{N}(s)}{ds} \right] ds, \quad (18)$$

where we assumed  $h_1 \equiv \tilde{b}(s)\lambda/\tilde{D}_e(s) = \text{constant}$ . The unknown variable  $\tilde{N}$  is embedded in the integrand of Eq. (18). To find  $\tilde{N}$  we may Laplace transform Eq. (18) and use the convolution theorem [12] to write

$$\tilde{N}(\omega) = \frac{2a^2 \bar{P} \hat{K}_2(a^2 \omega)}{\omega [1 + h_1 a^2 \omega \hat{K}_2(a^2 \omega)]} \quad (19)$$

with notation

$$\hat{f}(\omega) = \int_0^\infty e^{-\omega\tau} f(\tau) d\tau. \quad (20)$$

In Eq. (19)  $\hat{K}_2$ , which is the Laplace transform of the kernel  $K_2$  given by Eq. (12), is in the form

$$\hat{K}_2(\omega) = \frac{a}{\omega^2} (\sqrt{\omega} \coth(\sqrt{\omega}) - 1). \quad (21)$$

Relations (19) and (21) were derived earlier with slightly different convention in Forsberg and Massih [7]. Furthermore, in [7] the inverse Laplace transform of relation (19) was carried out to find the short-time and the long-time behaviour for  $\tilde{N}$ . Here, since our aim is to analyse the accuracy of our approximations, it is sufficient to note that according to Eq. (19) on identifying  $\hat{K}_2$ ,  $\hat{N}$  is determined uniquely for the given physical parameters,  $\bar{P}$ ,  $h_1$  and  $a$ . Hence by comparing the Laplace transform of Eq. (12) with Eq. (21) we can quantify the degree of our approximation. The Laplace transform of Eq. (12) is expressed as

$$\hat{K}_2(\omega) \approx \widehat{K}_2(\omega) = \frac{a}{3} \left( \frac{1}{\omega} - \frac{3}{4\pi} \sum_{i=1}^m \frac{A_i}{\omega + B_i} \right). \quad (22)$$

After determining the coefficients  $A_i$  and  $B_i$  we shall compare Eq. (21) with Eq. (22) to assess the level of our approximation.

#### 4. Analysis of error in approximate solution

The solution in Eq. (7) may be viewed as a functional of the form

$$\bar{\tau}([F, G]; \tau) = \frac{3}{4\pi} \int_0^\tau F\left(\frac{\tau-s}{a^2}\right) G(s) ds. \quad (23)$$

In the exact solution,  $F$  is given by the kernel  $K$  in Eq. (8) and  $G$  is given by the quantity  $P$ . In the approximate solutions (14) and (15),  $F$  is given by Eq. (13) and  $G$  is given by the respective (piecewise constant and piecewise linear) approximations of  $P$ .

In general, one may approximate  $K$  and  $P$  by writing

$$\tilde{K}(x) = K(x) + \varepsilon(x), \quad (24)$$

$$\tilde{P}(x) = P(x) + \eta(x), \quad (25)$$

where  $\varepsilon$  and  $\eta$  are the errors of the approximating functions. It should be noted that  $\eta(x)$  is time step size dependent and, at least in principle, can be made arbitrarily small by reducing the step size. We will therefore focus on the error in the calculated fission gas release, which originates from  $\varepsilon$  and assume that  $\eta = 0$ . The approximate solution to the diffusion equation, expressed in terms of fission gas release fraction, is

$$\begin{aligned} \Re([\tilde{K}, P]; \tau) &= \Re([K, P]; \tau) - \frac{3}{4\pi} \frac{\int_0^{\tau/a^2} \varepsilon(s) P(\tau - a^2 s) ds}{\int_0^{\tau/a^2} P(\tau - a^2 s) ds} \\ &= \Re([K, P]; \tau) - \frac{3}{4\pi} \bar{\varepsilon}([P(\tau - a^2 s)]; \tau/a^2), \end{aligned} \quad (26)$$

where  $\bar{\varepsilon}([P(\tau - a^2 s)]; \tau/a^2)$  denotes the weighted mean value of  $\varepsilon(s)$  in the interval  $[0, \tau/a^2]$  using  $P(\tau - a^2 s)$  as the weight function. In the special case that  $P(x) = P_0 = \text{constant}$ , we find

$$\Re([\tilde{K}, P]; \tau) = \Re([K, P]; \tau) - \frac{3}{4\pi} \bar{\varepsilon}(\tau/a^2), \quad (27)$$

where  $\bar{\varepsilon}(\tau/a^2)$  is the mean value of  $\varepsilon(s)$  in the interval  $[0, \tau/a^2]$ .

We can put an upper limit on the absolute error in the approximate solution. From Eq. (26) we obtain that the absolute error,  $|\Delta\Re|$ , takes the form

$$\begin{aligned} |\Delta\Re| &= \left| \frac{3}{4\pi} \bar{\varepsilon}([P(\tau - a^2 s)]; \tau/a^2) \right| \\ &= \frac{3}{4\pi} \left| \frac{\int_0^{\tau/a^2} \varepsilon(s) P(\tau - a^2 s) ds}{\int_0^{\tau/a^2} P(\tau - a^2 s) ds} \right|. \end{aligned} \quad (28)$$

If  $\sup(|\varepsilon(s)|) = |\varepsilon(\tau_0)| = \varepsilon_{\max}$ ,  $s \in [0, \tau/a^2]$  then we have

$$\max(|\Delta\Re|) = \left| \frac{3}{4\pi} \bar{\varepsilon}([\delta(s - \tau_0)]; \tau/a^2) \right| = \frac{3}{4\pi} \varepsilon_{\max}, \quad (29)$$

where  $\delta(\bullet)$  is a generalised function (for instance the Dirac delta function). The real irradiation histories never give rise to condition  $P(\tau) \propto \delta(\tau)$ , however, a sharp power transient may approach this situation.

From relations (27) and (29) we see that the maximum possible error (neglecting the error in  $P$ ) in the calculated fission gas release is larger for the time-dependent condition ( $P(t)$  not constant) than for the steady-state, i.e.,  $\varepsilon_{\max} \geq |\bar{\varepsilon}(\tau/a^2)|$ . This corollary has been quantified by exemplary calculations presented in Section 6. We may also conclude that a small error in the steady-state (Eq. (27)) does not ensure an equally small error under time-dependent conditions (Eq. (29)). Hence, steady-state conditions per se would not in general accurately quantify the degree of approximation made on  $\tilde{K}$ .

#### 5. Finding an approximate kernel

In the previous section we showed that in order to estimate the error in calculated fission gas release which originates from the approximation of the kernel,  $K$ , we need to know the quantity  $P$ . Therefore, the problem of finding the coefficients  $A_i$  and  $B_i$ , and determining the number of terms,  $m$ , in Eq. (13), which yield sufficient accuracy in the calculated fission gas release, is dependent on the  $P$ 's. For instance, in order to minimise the maximum absolute error in fission gas release for constant  $P$  we should according to Eq. (27) try to minimise  $\sup(|\bar{\varepsilon}(s)|)$ . For completely arbitrary  $P$ , on the other hand, we should according to Eq. (29) minimise the norm of  $\varepsilon$  given by

$$\|\varepsilon\|_\infty = \sup(|\varepsilon(s)|) = \sup(|\tilde{K}(s) - K(s)|) \quad (30)$$

for  $s$  in some interval  $[0, \tau_{\max}]$ . Minimising the norm defined in Eq. (30) should be compared to minimising the norm expressed as

$$\|\varepsilon\|_2 = \sqrt{\int_0^{\tau_{\max}} \varepsilon(s)^2 ds} = \sqrt{\int_0^{\tau_{\max}} (\tilde{K}(s) - K(s))^2 ds} \quad (31)$$

which, in a discrete form, is equivalent to the least-square method (using a set of equidistant  $s$  values). It is

therefore clear that the ordinary least-square method does not provide a fit that in general would minimise the absolute error in fission gas release. However, minimising Eq. (30) is more difficult than minimising Eq. (31). Here we try to minimise Eq. (30) by introducing a weight function  $w(s)$  ( $w(s) > 0$ ) as follows:

$$\begin{aligned} \|\varepsilon\|_{2w} &= \sqrt{\int_0^{\tau_{\max}} w(s)\varepsilon(s)^2 ds} \\ &= \sqrt{\int_0^{\tau_{\max}} w(s)\left(\tilde{K}(s) - K(s)\right)^2 ds}. \end{aligned} \tag{32}$$

The weight function  $w(s)$  is chosen in order to give a small  $\sup(|\tilde{K}(s) - K(s)|)$ . No attempt has been made to optimise the choice of  $w$  but we have selected (for  $\tilde{K}$  given by Eq. (13))  $w(s - \delta) \approx (dl/ds)^2 = 1 + (dK(s)/ds)^2$  where  $\delta$  is a small number and  $l(s)$  is the length of the parameterised curve  $C : \mathbf{r}(s) = (s, K(s))$ ,  $s \in [0, \tau_{\max}]$ . This choice (which gives a higher weight to points close to zero) somewhat compensates for the problem in the fitting of Eq. (13), which originates from the fact that  $dK(s)/ds \rightarrow -\infty$  as  $s \rightarrow 0^+$ . In the numerical implementation of this method, as in Lassmann and Benk [9], we also impose the constraint  $\sum_{i=1}^m A_i = 4\pi/3$  on the coefficients  $A_i$  in Eq. (13). This constraint is obtained by matching Eq. (8) with Eq. (13) and using the identity  $\sum_{k=1}^{\infty} k^{-2} = \pi^2/6$ .

**6. Examples and test cases**

*6.1. Approximate kernels*

Using the minimisation method presented in Section 5 in the interval  $[0, \tau_{\max} = 0.5]$  and five terms ( $m = 5$ ) in Eq. (13) we obtain the following values for the coefficients  $A_i$  and  $B_i$ :

$$\begin{pmatrix} A_1 \\ A_2 \\ A_3 \\ A_4 \\ A_5 \end{pmatrix} = \begin{pmatrix} 0.906322 \\ 0.432587 \\ 0.0501351 \\ 0.170014 \\ 2.6297321 \end{pmatrix}, \quad \begin{pmatrix} B_1 \\ B_2 \\ B_3 \\ B_4 \\ B_5 \end{pmatrix} = \begin{pmatrix} 57.4131 \\ 387.104 \\ 162769 \\ 4410.53 \\ 10.0492 \end{pmatrix}. \tag{33}$$

Fig. 1 shows the difference between the approximate and exact kernels  $\varepsilon(x) \equiv \tilde{K}(x) - K(x)$  versus  $x$  for two different scales in  $x$ . From the figure we see that  $\sup(|\varepsilon(s)|) \approx 0.006$  and therefore, according to Eq. (29), we should have  $\max(|\Delta\mathcal{R}|) \approx (3/4\pi)0.006 \approx 0.0014$ . This means that we do not expect the error in the calculated fission gas release fraction (emanating from the approximation of  $K$ ) to exceed 0.0014.

Using our fitting method in the interval  $[0, \tau_{\max} = 0.5]$  and four terms ( $m = 4$ ) in Eq. (13) we obtain the following values for the coefficients  $A_i$  and  $B_i$ :

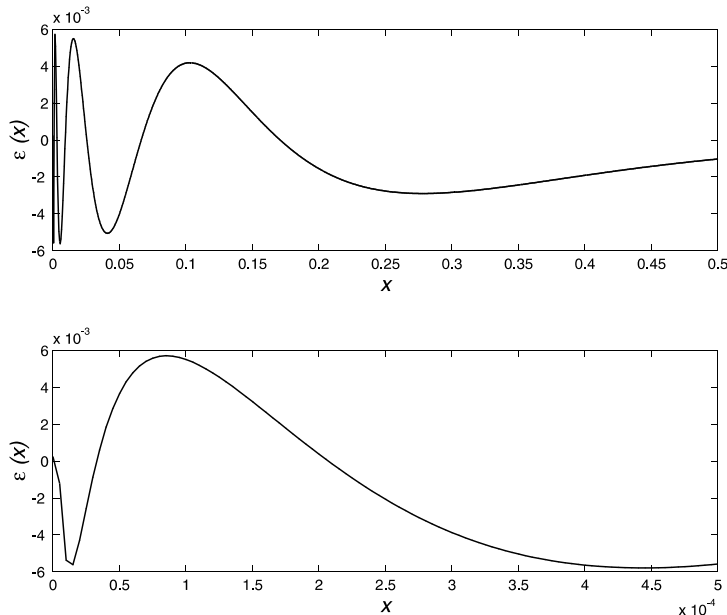


Fig. 1. The difference between the approximate and the exact kernel,  $\varepsilon(x) = \tilde{K}(x) - K(x)$ , versus  $x$  in the intervals:  $[0, 0.5]$  and  $[0, 0.0005]$ .  $\tilde{K}(x)$  is calculated by relation (13) with  $m = 5$  according to Eq. (33) while  $K(x)$  is evaluated using Eq. (8) with ( $k = 1, 2, \dots, 10^4$ ).

$$\begin{pmatrix} A_1 \\ A_2 \\ A_3 \\ A_4 \end{pmatrix} = \begin{pmatrix} 0.969892 \\ 0.397287 \\ 0.118500 \\ 2.7031112 \end{pmatrix}, \quad \begin{pmatrix} B_1 \\ B_2 \\ B_3 \\ B_4 \end{pmatrix} = \begin{pmatrix} 72.5968 \\ 796.773 \\ 29083.0 \\ 10.2469 \end{pmatrix}. \tag{34}$$

Fig. 2 shows  $\varepsilon(x) \equiv \tilde{K}(x) - K(x)$  versus  $x$  for two different scales in  $x$ . From the figure we notice that  $\sup(|\varepsilon(s)|) \approx 0.014$  and thus, according to Eq. (29), we should have  $\max(|\Delta\mathfrak{R}|) \approx (3/4\pi)0.014 \approx 0.0033$ . This means that we do not expect the error in calculated fission gas release fraction (originating from the approximation of  $K$ ) to exceed 0.0033.

We should remark that for the case of intergranular gas release (Cauchy boundary condition) the same coefficients (33) and (34) prevail. This is because the same kernel governs the kinetics of the process, cf. relations (11) and (18). For example, the quantities of interest for this problem are the intergranular gas density (per unit volume)  $C_b = 3N/2a$  and the intragranular gas density defined by the relation:  $C_0(\tau) = \int_0^a 4\pi r^2 [c(r, \tau) - c(a, \tau)] dr$ . As shown in [7] the kinetics of these quantities, for  $h_1 \equiv \tilde{b}(s)\lambda/\tilde{D}_c(s) = \text{constant}$ , can be described by

$$C_b(\tau) = \int_0^\tau \frac{3}{a} K_2\left(\frac{\tau-s}{a^2}\right) q(s) ds, \tag{35}$$

$$C_0(\tau) = \int_0^\tau \left[ 1 - \frac{3}{a} K_2\left(\frac{\tau-s}{a^2}\right) \right] q(s) ds, \tag{36}$$

where

$$q(s) = P(s) - \frac{ah_1}{3} \frac{dC_b(s)}{ds}. \tag{37}$$

Thus the kernel appearing in the integrand of Eq. (36) can be approximated as

$$1 - \frac{3}{a} K_2(x) \approx \sum_{i=1}^m \frac{3}{4\pi} A_i e^{-B_i x} \tag{38}$$

and so forth (where to obtain relation (38) we utilized Eqs. (12) and (13)).

It should be noted that the error estimates presented in Section 4 are derived for the case of Dirichlet boundary condition and that we have not derived similar error estimates for the case of Cauchy boundary condition. However, for a small grain boundary resolution ( $h_1$  sufficiently small) we see from Eqs. (35) and (37) that the error estimates in Eqs. (27) and (29) are approximately valid also for the Cauchy boundary condition.

### 6.2. Results for steady-state

For constant conditions ( $P(s) = P_0 = \text{constant}$ ) we compare the exact solution for the gas release fraction given by Eq. (16) with the associating approximate solution given by Eq. (17) using  $\bar{P} = P_0$  and the coefficients given in Eq. (33) (i.e.  $m = 5$ ). The comparison is depicted in Fig. 3. Fig. 4 shows the difference between the two solutions, i.e.,  $\Delta(x) \equiv \mathfrak{R}(x) - \mathfrak{R}(x)$  versus  $x \equiv \tau/a^2$ . From

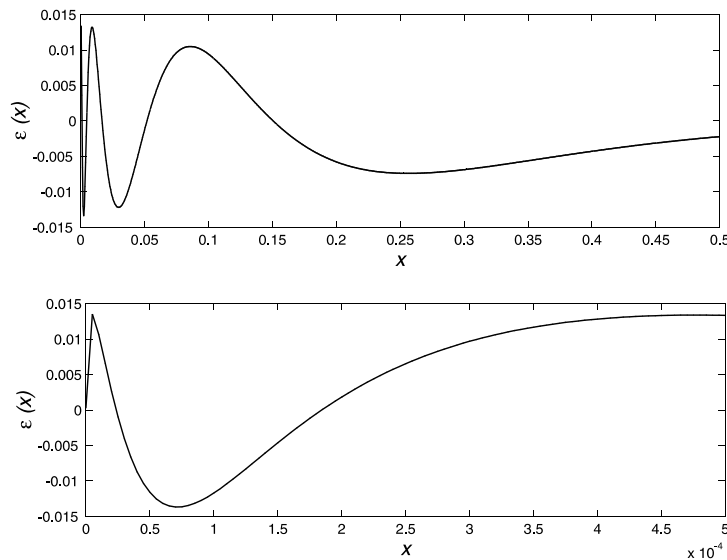


Fig. 2. The difference between the approximate and the exact kernel,  $\varepsilon(x) = \tilde{K}(x) - K(x)$ , versus  $x$  in the intervals:  $[0, 0.5]$  and  $[0, 0.0005]$ .  $\tilde{K}(x)$  is calculated by relation (13) with  $m = 4$  according to Eq. (34) while  $K(x)$  is evaluated using Eq. (8) with ( $k = 1, 2, \dots, 10^4$ ).

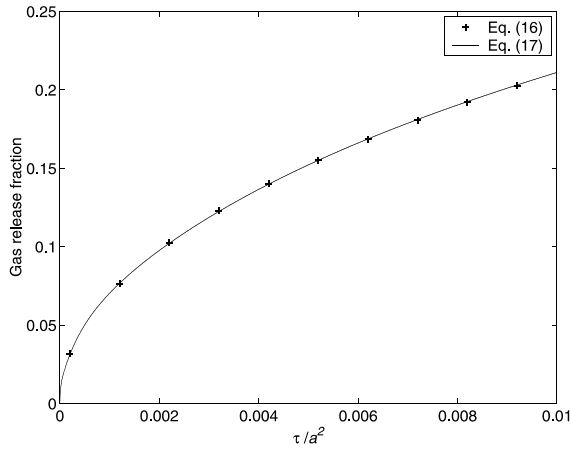


Fig. 3. Gas release fraction  $\mathfrak{R}$  as a function of ‘time’ is calculated using the approximate relation (17) with the coefficients according to Eq. (33) versus the exact solution Eq. (16) with  $(k = 1, 2, \dots, 10^4)$  for  $\mathfrak{R} < 0.2$ .

Fig. 4 we can deduce that the accuracy of the algorithm is good for constant conditions and that the maximum error is less than 0.0014, or  $\sup(|\Delta(s)|) < 0.014$ , which is consistent with our results in Sections 4 and 6.1.

Comparing the exact solution in Eq. (16) with the approximate solution in Eq. (17) using  $\bar{P} = P_0$  and the coefficients given in Eq. (34) we obtain the result for  $\Delta(x)$  versus  $x$  shown in Fig. 5. From Fig. 5 we notice that the accuracy of the approximate algorithm is quite good and that the maximum error is less than 0.0033,

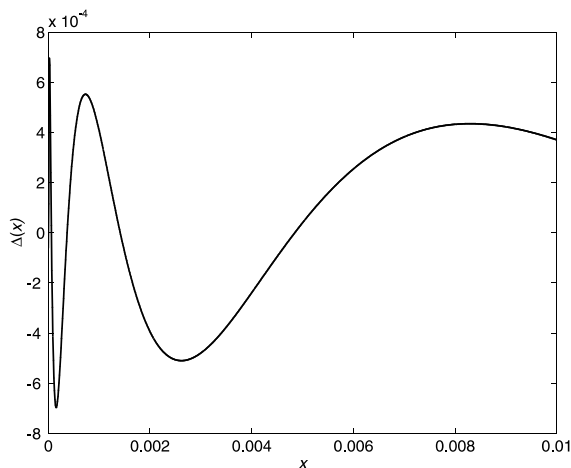


Fig. 4. The difference between the approximate and the exact gas release fraction,  $\Delta(x) \equiv \mathfrak{R}(x) - \mathfrak{R}(x)$  versus  $x \equiv \tau/a^2$  for  $\mathfrak{R} < 0.2$ .  $\mathfrak{R}(x)$  is calculated by using relation (17) with  $m = 5$  according to Eq. (33) while  $\mathfrak{R}(x)$  is evaluated using relation (16) with  $(k = 1, 2, \dots, 10^4)$ .

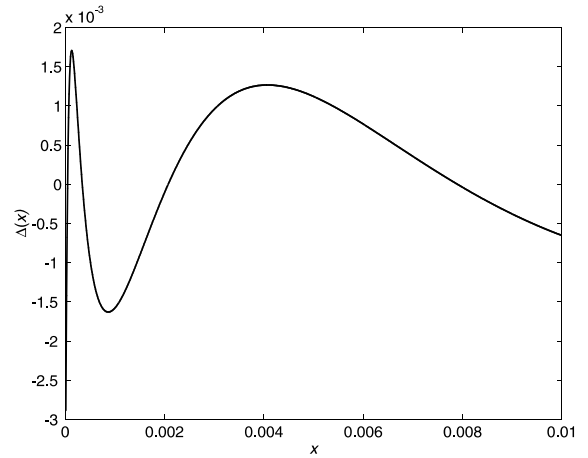


Fig. 5. The difference between the approximate and the exact gas release fraction,  $\Delta(x) \equiv \mathfrak{R}(x) - \mathfrak{R}(x)$  versus  $x \equiv \tau/a^2$  for  $\mathfrak{R} < 0.2$ .  $\mathfrak{R}(x)$  is calculated by using relation (17) with  $m = 4$  according to Eq. (34) while  $\mathfrak{R}(x)$  is evaluated using relation (16) with  $(k = 1, 2, \dots, 10^4)$ .

$\sup(|\Delta(s)|) < 0.0033$ , which is consistent with our results in Sections 4 and 6.1.

### 6.3. Results for the intergranular gas

Finally, we compare the exact expression (21) and the associating approximate relation (22) for the Laplace transform of the kernel  $K_2$  given by Eq. (12). This kernel appears in the calculation of the intergranular gas release according to Forsberg and Massih [7]. Fig. 6 shows the difference between the approximate kernel and exact

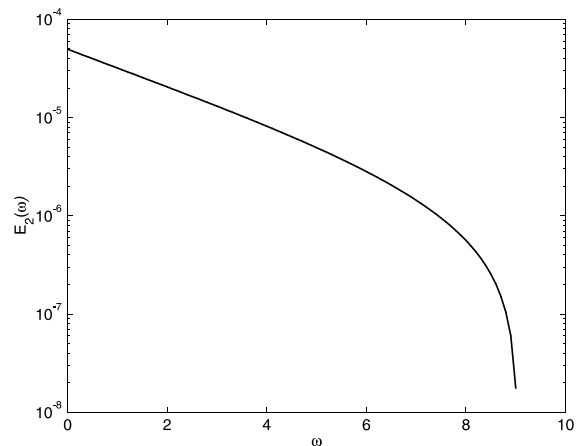


Fig. 6. The difference between the approximate and the exact kernel in  $\omega$ -space,  $E_2(\omega) \equiv (\widehat{K}_2(\omega) - \widehat{K}_2(\omega))/a$ .  $\widehat{K}_2(\omega)$  is calculated by using relation (22) with  $m = 5$  according to Eq. (33) while  $\widehat{K}_2(\omega)$  is evaluated using relation (21).

kernel  $E_2(\omega) \equiv (\widehat{K}_2(\omega) - \check{K}_2(\omega))/a$  versus  $\omega$  using the coefficients given in Eq. (33). As can be seen from this figure  $\sup(|E_2(s)|) \approx 5 \times 10^{-5}$ .

## 7. Closure

In this note we have analysed the accuracy of a numerical method of Forsberg and Massih for calculating fission gas release fractions. We have presented some results, which give an estimate of the maximum absolute error in the calculated fission gas release. A new approximation of the coefficients in the kernel is also presented which gives satisfactory accuracy in the calculated fission gas release for both low and high release regimes.

The analysis by Elton and Lassmann [8] shows that the original approximate kernel in the Forsberg–Massih algorithm [6] results in a maximum absolute error (at low release) of about 0.02. The present analysis shows that the maximum absolute error (using the new fitting method and one extra term,  $m = 4$ , in the approximate kernel) can be reduced to 0.0034. This is in concordance with recent calculations of Lassmann [13], where a better fitting of the new FORMAS algorithm (cf. Section 1) improved the accuracy of the algorithm. The new FORMAS algorithm according to Lassmann is simple, fast, robust, insensitive to time step lengths and

well balanced over the entire range of fission gas release [13].

## References

- [1] NEA Nuclear Science Task Force, Scientific issues in fuel behaviour, OECD document, nea0213-fuel.pdf. Available from <[www.nea.fr/html/pub/webpubs/](http://www.nea.fr/html/pub/webpubs/)>.
- [2] K. Lassmann, J. Nucl. Mater. 101 (1992) 259.
- [3] G.A. Berna, C.E. Beyer, K.L. Davis, D.D. Lanning, FRAPCON-3: A computer code for the calculation of steady-state, thermal-mechanical behavior of oxide fuel rods for high burnup, Report NUREG/CR-6534, 1997.
- [4] L.D. Noble, C.S. Rim, Report NUREG/CR-2507, 1982.
- [5] J.R. Matthews, M.H. Wood, Nucl. Eng. Des. 56 (1980) 439.
- [6] K. Forsberg, A.R. Massih, J. Nucl. Mater. 127 (1985) 141.
- [7] K. Forsberg, A.R. Massih, J. Nucl. Mater. 135 (1985) 140.
- [8] P.T. Elton, K. Lassmann, Nucl. Eng. Des. 101 (1987) 259.
- [9] K. Lassmann, H. Benk, J. Nucl. Mater. 280 (2000) 127.
- [10] M.V. Speight, Nucl. Sci. Eng. 37 (1969) 180.
- [11] Y. Choquet-Bruhat, C. De Witt-Morette, M. Dillard-Bleick, Analysis, Manifold and Physics, North-Holland, Amsterdam, 1977.
- [12] M. Abramowitz, I.A. Stegun, Handbook of Mathematical Functions, Dover, New York, 1972.
- [13] K. Lassmann, Numerical algorithms for intragranular diffusional release incorporated in the TRANSURANUS code, in: Fission Gas Behaviour in Water Reactor Fuels, Seminar Proceedings, Cadarache, France, 26–29 September, 2000, p. 499.